

Supporting Information

for

Step-Edge Self-Assembly During Graphene Nucleation on a Nickel Surface: QM/MD Simulations

Ying Wang,^{1,2*} Alister J. Page,^{3*†} Hai-Bei Li,^{4*} Hu-Jun Qian,⁵ Meng-gai Jiao,¹ Zhi-jian Wu,¹
Keiji Morokuma,^{**4} and Stephan Irle^{**2}

¹*State Key Laboratory of Rare Earth Resource Utilization, Changchun Institute of Applied
Chemistry, Chinese Academy of Sciences, Changchun, 130022, China*

²*WPI-Institute of Transformative Bio-Molecules and Department of Chemistry, Graduate
School of Science, Nagoya University, Nagoya 464-8602, Japan*

³*Discipline of Chemistry, School of Environmental and Life Sciences, The University of
Newcastle, Callaghan 2308, Australia*

⁴*Fukui Institute for Fundamental Chemistry, Kyoto University, Kyoto, 606-8103, Japan*

⁵*Institute of Theoretical Chemistry, State Key Laboratory of Theoretical and
Computational Chemistry, Jilin University, Changchun 130023, China*

Computational method

Fig.S1: Last snapshots of ten trajectories A1-A10 at 65 ps for 53C (model A)

Fig.S2: Last snapshots of ten trajectories B1-B10 at 65 ps for 72C (model B)

Fig.S3: Last snapshots of ten trajectories C1-C10 at 65 ps for 96C (model C)

Fig.S4: For Model A, a-b) averaged populations of spⁿ-hybridized carbon atoms including Ni-C and without Ni-C; c) averaged evolution of carbon cluster sizes; d) average carbon ring populations, during 65 ps graphene nucleation process. All data averaged over ten trajectories.

Fig.S5: For Model B, a-b) averaged populations of spⁿ-hybridized carbon atoms including

Ni-C and without Ni-C; c) averaged evolution of carbon cluster sizes; d) average carbon ring populations, during 65 ps graphene nucleation process. All data averaged over ten trajectories.

Fig.S6: For Model C, a-b) averaged populations of sp^n -hybridized carbon atoms including Ni-C and without Ni-C; c) averaged evolution of carbon cluster sizes; d) average carbon ring populations, during 65 ps graphene nucleation process. All data averaged over ten trajectories.

Movie M1: Step-edge formation self-assembly observed in trajectory A1. Brown and blue spheres represent Ni and C atoms, respectively. Each frame represents 0.8 ps.

Computational method

The quantum chemical molecular dynamics (QM/MD) simulations in this work were performed using the self-consistent charge (SCC) density functional tight-binding (DFTB) method, in conjunction with Ni-C parameters developed previously within our group. The DFTB method is a valence-only extended Hückel method, and therefore explicitly includes contributions from carbon $2s$ and $2p$ orbitals, and nickel $3d$ and $4s$ orbitals. A finite electronic temperature, T_e , of 3,000 K was adopted to alleviate SCC convergence issues. Molecular orbital occupations near the Fermi level were therefore described by a Fermi-Dirac distribution function (and could vary continuously over the interval $[0,2]$). Such an approach has been used and validated by us in previous investigations of transition-metal catalyzed single-walled CNT (SWCNT) nucleation and growth.^{1,2} DFTB energy and gradients were computed ‘on-the-fly’ at each step of the MD simulation, the latter of which employed the velocity-Verlet algorithm ($\Delta t = 1$ fs) for time propagation. The nuclear temperature, T_n , was held constant at 1,180 K for all simulations with a Nosé-Hoover chain thermostat (chain length = 3).

All simulations reported here employ a model $6 \times 6 \times 4$ Ni(111) surface (144 Ni atoms in total). The bottom Ni layer was held stationary throughout, thereby approximating the underlying bulk region. Periodic boundary conditions for this large unit cell were enforced under the Γ point approximation, and the pristine Ni(111) surface was initially equilibrated for 10 ps at 1,180 K; in this run the bcc lattice was maintained perfectly. Carbon dissolution was then simulated by the addition of carbon atoms into randomly selected interstitial sites in the Ni(111) subsurface at intervals of 0.5 ps, as previously implemented for nonequilibrium carbon supply during the MD simulation.³ Initial velocities of each newly added carbon atom were drawn from a Maxwell-Boltzmann distribution at T_n . To establish the role of carbon density in SLG versus MLG growth, we simulate graphene growth as described above using three different subsurface carbon densities ~ 37 , 50 and 66 atom % (53, 72 and 96 total carbon atoms, respectively). These densities correspond to 74, 100 and 133 % of the carbon required to form continuous SLG for a model system of this size. Following the initial period of carbon atom addition, each system was annealed at constant temperature for 65 ps. We note finally that for each simulation condition, 10 independent

QM/MD trajectories were computed. These trajectories for the 37, 50 and 66 atom % simulations are denoted as A_n , B_n , and C_n ($n = 1, 2, \dots, 10$), respectively.

References

- (1) Page, A. J.; Ohta, Y.; Okamoto, Y.; Irle, S.; Morokuma, K. Defect Healing during Single-Walled Carbon Nanotube Growth: A Density-Functional Tight-Binding Molecular Dynamics Investigation. *J. Phys. Chem. C* 2009, *113*, 20198-20207
- (2) Page, A. J.; Ohta, Y.; Irle, S.; Morokuma, K. Mechanisms of Single-Walled Carbon Nanotube Nucleation, Growth and Healing Determined Using QM/MD Methods *Acc. Chem. Res.* 2010, *43*, 1375-1385
- (3) Li, H.-B.; Page, A. J.; Wang, Y.; Irle, S.; Morokuma, K. Sub-surface nucleation of graphene precursors near a Ni(111) step-edge. *Chemical Communications* 2012, *48*, 7937-7939

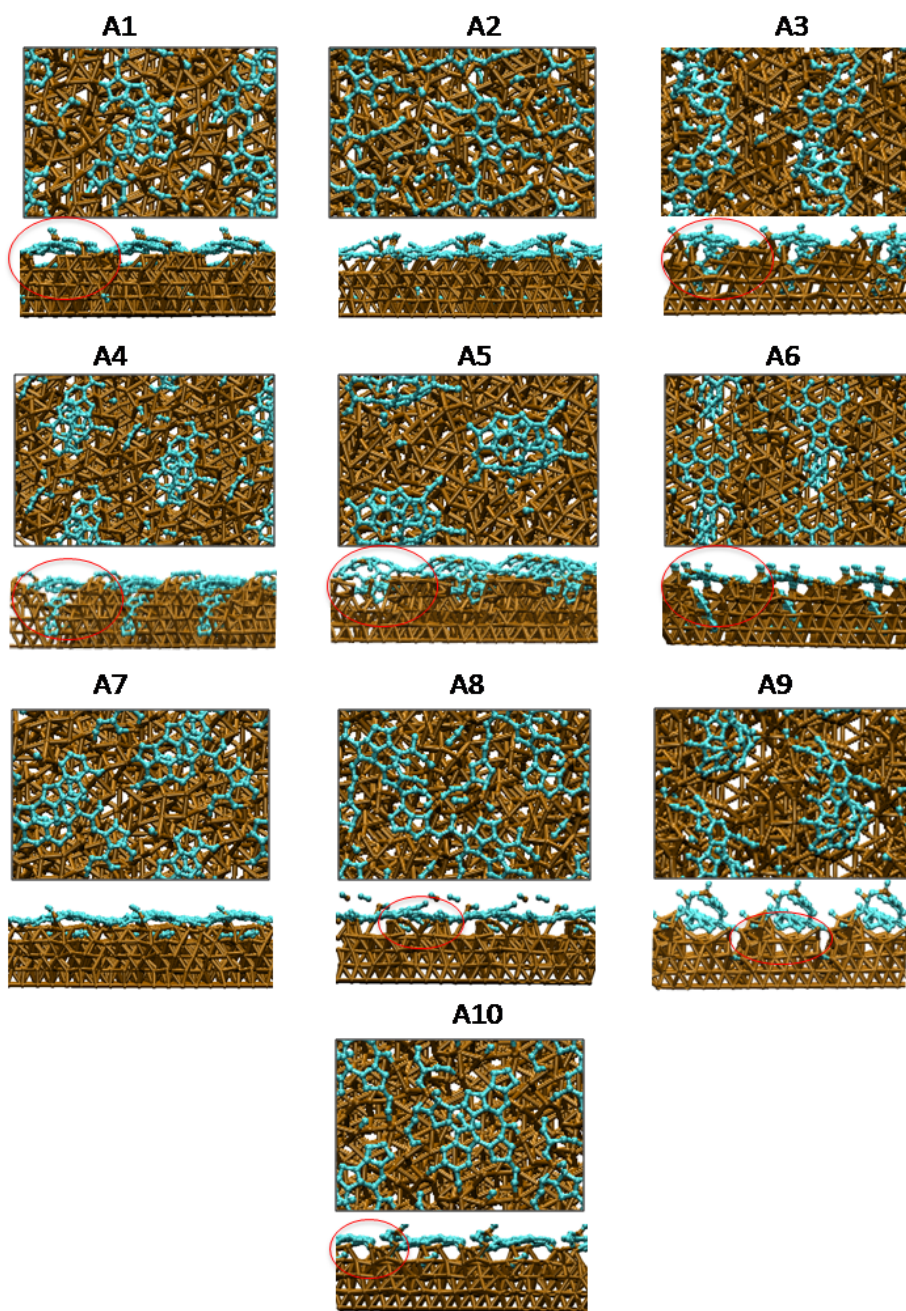


Fig. S1: Last snapshots of ten trajectories A1-A10 at 65 ps for 53C (model A).

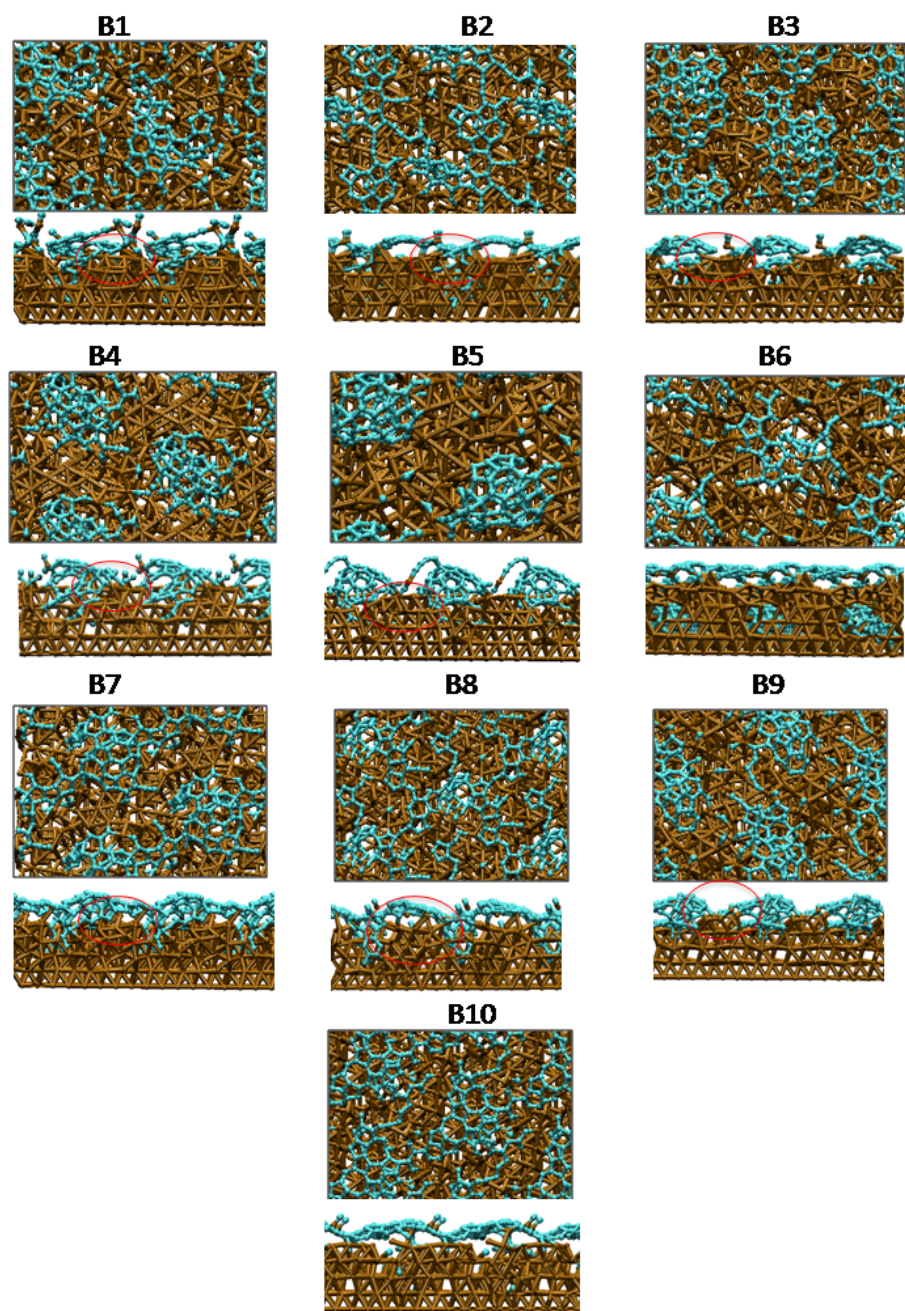


Fig. S2: Last snapshots of ten trajectories B1-B10 at 65 ps for 72C (model B).

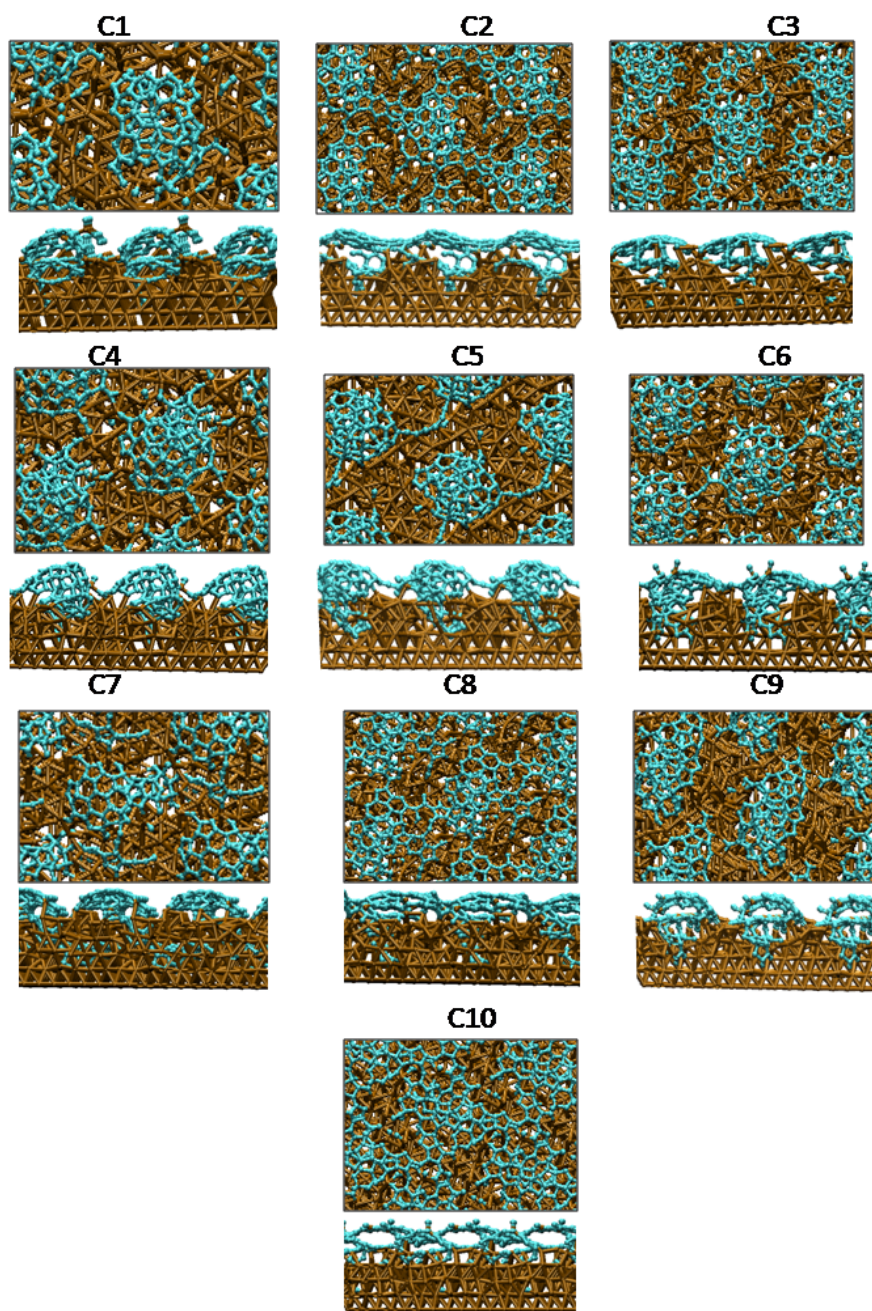


Fig. S3: Last snapshots of ten trajectories C1-C10 at 65 ps for 96C (model C).

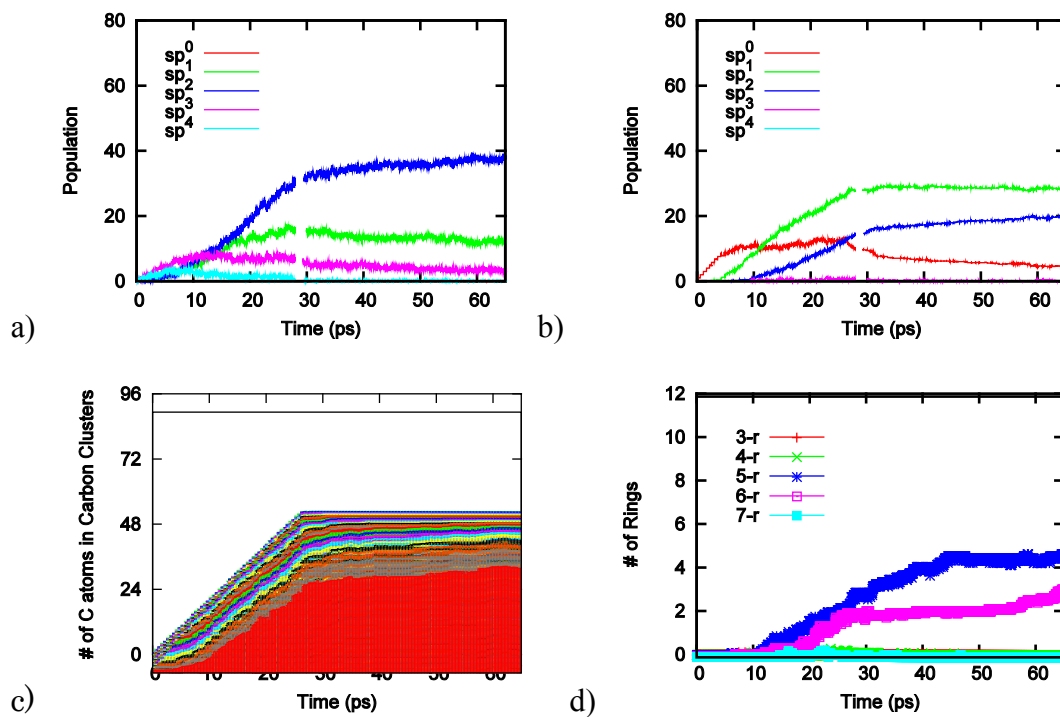


Fig. S4 For Model A, a-b) averaged populations of sp^n -hybridized carbon atoms including Ni-C and without Ni-C; c) averaged evolution of carbon cluster sizes; d) average carbon ring populations, during 65 ps graphene nucleation process. All data averaged over ten trajectories.

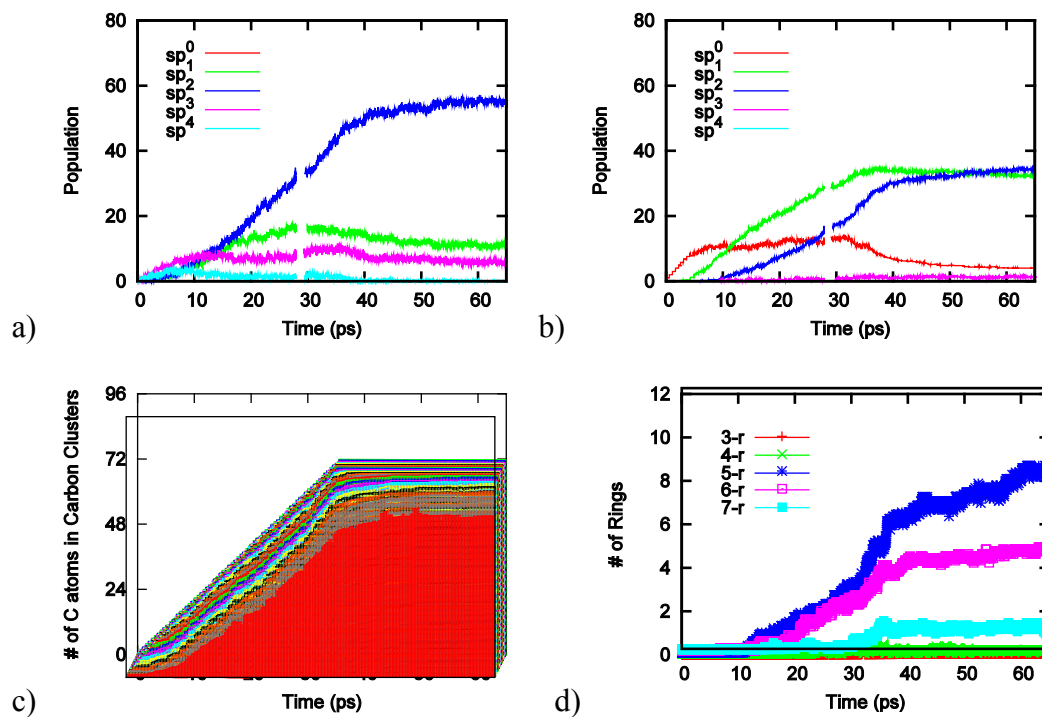


Fig. S5: For Model B, a-b) averaged populations of sp^n -hybridized carbon atoms including Ni-C and without Ni-C; c) averaged evolution of carbon cluster sizes; d) average carbon ring populations, during 65 ps graphene nucleation process. All data averaged over ten trajectories.

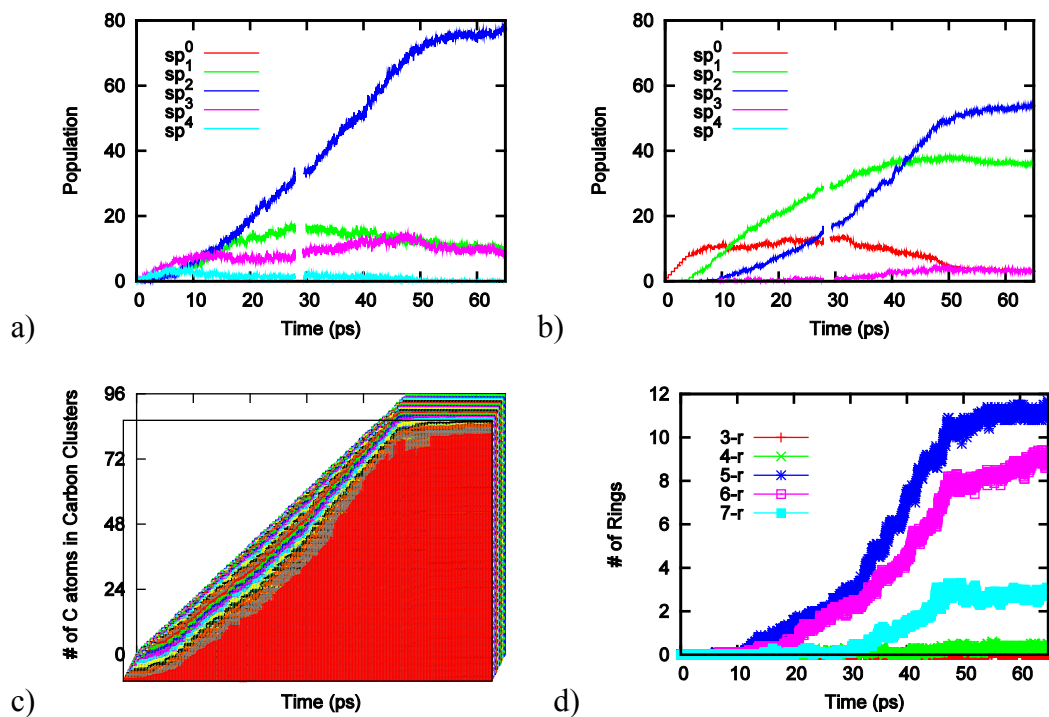


Fig. S6: For Model C, a-b) averaged populations of sp^n -hybridized carbon atoms including Ni-C and without Ni-C; c) averaged evolution of carbon cluster sizes; d) average carbon ring populations, during 65 ps graphene nucleation process. All data averaged over ten trajectories.